Supporting Information

Electric Fano resonance-based terahertz metasensors

Ride Wang,[a] Lei Xu,[b] Jiayi Wang,[c] Lang Sun,[a] Yanan Jiao,[d] Yuan Meng,[e] Shuo Chen,[a] Chao Chang,[*a,f] and Chunhai Fan[*g]

[a]*Innovation Laboratory of Terahertz Biophysics, National Innovation Institute of Defense Technology, Beijing, 100071, China. E-mail: gwyzlzssb@pku.edu.cn*

[b]*Advanced Optics and Photonics Laboratory, Department of Engineering, School of Science and Technology, Nottingham Trent University, Nottingham NG11 8NS, UK.*

[c]*Key Laboratory of Weak-Light Nonlinear Photonics, Ministry of Education, TEDA In-stitute of Applied Physics and School of Physics, Nankai University, Tianjin 300457, China.*

[d]*Department of General Surgery, First Medical Center of Chinese PLA General Hospital, Beijing 100853, People's Republic of China.*

[e]*Key Laboratory of Photonics Control Technology of the Ministry of Education, Tsinghua University.*

[f]*School of Physics, Peking University, Beijing, 100871, China.*

[g]*School of Chemistry and Chemical Engineering Shanghai Jiao Tong University Shang-hai 200240, China. E-mail: fchh@sinap.ac.cn*

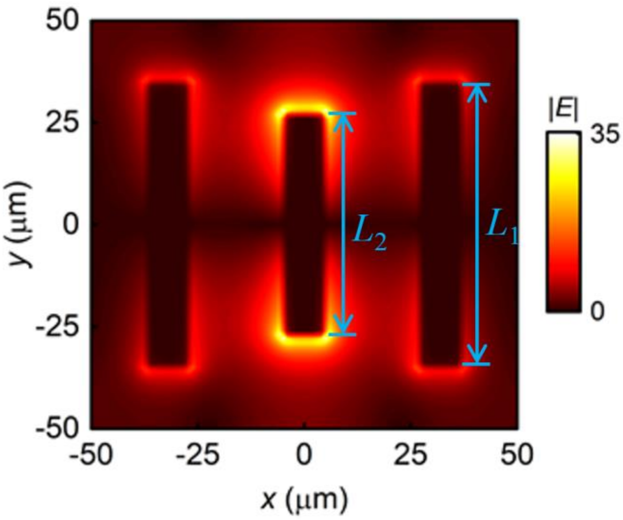

Figure S1 Based on the electric near-field distribution, a significant enhancement of the electric field (with more than 35-fold at the maximum position) at the resonance frequency point with L_2 = 55 μm.

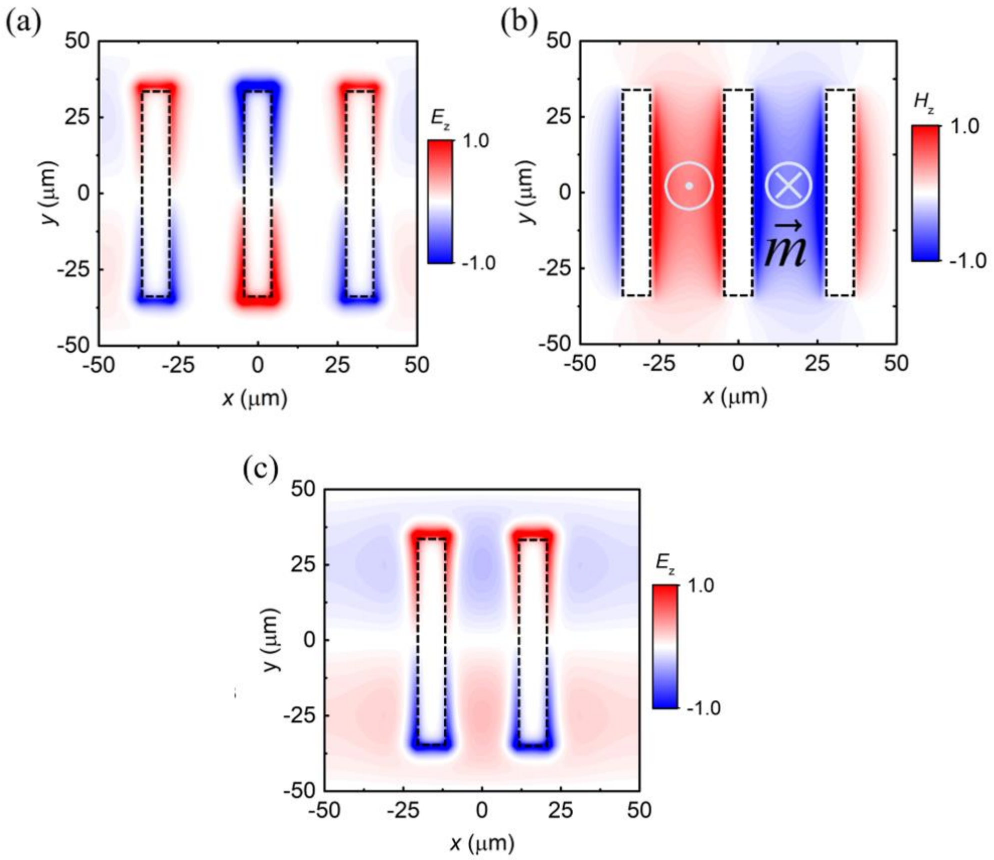

Figure S2 (a, b) Distribution of electric and magnetic field components for bound states in the continuum (BIC). (c) The E_z distribution of the dimer microrods with the same size as a contrast.

The defined building blocks of the metasurface is to be gold microrods trimer with adjustable mid-microrod length to enhance the near-filed amplitude of the Fano resonance. In the resonator, the electric and magnetic field distribution of the symmetry-protected BIC mode can be observed directly in the Figure S2(a,b), which is superior to the dimer microrods in the literature in the Figure S2(c). More importantly, one can find that the electric and magnetic field distributions of the BIC and quasi-BIC are similar by comparing Figure S2(a,b) and Figure 2(c,d), which indicate the quasi-BIC resonance inherits the BIC and Fano resonance is BIC-inspired.

In the section, we would introduce the multipoles scattering method in detail. Electric Fano resonance is formed by the destructive interference between a leaky electric dipole resonance and a bounded toroidal dipole mode, thus resulting in the sharp resonance. Furthermore, to quantitatively analyze the cause of forming this high Q resonance, we integrate the electric current density over the surface of the PEC microrods through simulation. The obtained surface current describes the effective current that creates the scattered field from our PEC microrods. [a, b] We then perform the spherical multipolar decomposition using these calculated surface currents and obtained the contributions from different multipolar components. [c] Furthermore, based on the obtained current, we perform the Cartesian multipolar decomposition to obtain the contributions of electric dipole mode and toroidal dipole mode. [d] The following representations of the multipole distribution are based on the Cartesian basis ($\alpha, \beta = x, y, z$). [e, f]

$$I = \frac{2w^4}{3c^3}\left|\vec{P}\right|^2 + \frac{2w^4}{3c^3}\left|\vec{M}\right|^2 + \frac{2w^6}{3c^5}\left|\vec{T}\right|^2 + \frac{w^6}{5c^5}\left|\vec{Q}_e\right|^2 + \frac{w^6}{20c^5}\left|\vec{Q}_m\right|^2 \tag{S1}$$

$$\vec{P} = \frac{1}{iw}\int d^3r\vec{J} \tag{S2}$$

$$\vec{M} = \frac{1}{2c}\int d^3r(\vec{r}\times\vec{J}) \tag{S3}$$

$$\vec{T} = \frac{1}{10c}\int d^3r[(\vec{r}\cdot\vec{J})r - 2r^2J] \tag{S4}$$

$$\vec{Q}_e = \frac{1}{2iw}\int d^3r[r_\alpha J_\beta + r_\beta J_\alpha - \frac{2}{3}\delta_{\alpha\beta}(\vec{r}\cdot\vec{J})] \tag{S5}$$

$$\vec{Q}_m = \frac{1}{3c}\int d^3r[(\vec{r}\times\vec{J})_\alpha r_\beta + (\vec{r}\times\vec{J})_\beta r_\alpha] \tag{S6}$$

Where J is the surface current density, c is the speed of light in vacuum and $\vec{r}$ is the displacement vector. We used the charge conservation relation $iw\rho + \nabla\cdot\vec{J} = 0$ to eliminate the charge density (ρ) in favor of current density (J) in the electric dipole and quadrupole.

[a] Mishchenko, M. I., L. D. Travis and A. A. Lacis (2002). Scattering, Absorption, and Emission of Light by Small Particles. NASA Goddard Institute for Space Studies, New York Institute for Space Studies, New York Pace Studies, New York New York, 1–486.

[b] Jackson, J. D. (1998). Classical Electrodynamics. American Journal of Physics, 808.

[c] Grahn P, Shevchenko A, Kaivola M. Electromagnetic multipole theory for optical nanomaterials. New Journal of Physics, 2012, 14(14):658-666.
[d] Gurvitz, E. A.; Ladutenko, K. S.; Dergachev, P. A.; Evlyukhin, A. B.; Miroshnichenko, A. E.; Shalin, A. S., The high-order toroidal moments and anapole states in all-dielectric photonics. Laser & Photonics Reviews 2019, 13 (5), 1800266.
[e] Chen, X.; Fan, W.; Yan, H., Toroidal dipole bound states in the continuum metasurfaces for terahertz nanofilm sensing. Optics Express 2020, 28 (11), 17102-17112.
[f] Han, S.; Cong, L.; Gao, F.; Singh, R.; Yang, H., Observation of Fano resonance and classical analog of electromagnetically induced transparency in toroidal metamaterials. Annalen der Physik 2016, 528 (5), 352-357.